Natural mutations in *IFITM3* modulate post-translational regulation and toggle antiviral specificity

Alex A Compton[1,*], Nicolas Roy[1], Françoise Porrot[1], Anne Billet[1], Nicoletta Casartelli[1], Jacob S Yount[2], Chen Liang[3] & Olivier Schwartz[1,4,5,**]

Abstract

The interferon-induced transmembrane (IFITM) proteins protect host cells from diverse virus infections. IFITM proteins also incorporate into HIV-1 virions and inhibit virus fusion and cell-to-cell spread, with IFITM3 showing the greatest potency. Here, we report that amino-terminal mutants of IFITM3 preventing ubiquitination and endocytosis are more abundantly incorporated into virions and exhibit enhanced inhibition of HIV-1 fusion. An analysis of primate genomes revealed that *IFITM3* is the most ancient antiviral family member of the *IFITM* locus and has undergone a repeated duplication in independent host lineages. Some *IFITM3* genes in nonhuman primates, including those that arose following gene duplication, carry amino-terminal mutations that modify protein localization and function. This suggests that "runaway" IFITM3 variants could be selected for altered antiviral activity. Furthermore, we show that adaptations in *IFITM3* result in a trade-off in antiviral specificity, as variants exhibiting enhanced activity against HIV-1 poorly restrict influenza A virus. Overall, we provide the first experimental evidence that diversification of *IFITM3* genes may boost the antiviral coverage of host cells and provide selective functional advantages.

Introduction

Viruses depend on numerous cellular factors and pathways to complete the viral life cycle and spread to new target cells. Known as virus cofactors, these are host molecules that are commandeered by the virus in order to promote efficient infection [1]. To prevent virus takeover, cells express a battery of antiviral effectors that repress viral replication at multiple stages. These proteins make up the cell-intrinsic innate immune response and are also known as host restriction factors. The establishment of a hostile intracellular environment sets the stage for ongoing host–virus coevolution, a phenomenon that is particularly well characterized between primates and lentiviruses [2]. As their name implies, host restriction factors influence the host tropism of virus infections *in vitro* and *in vivo* because they are rapidly evolving and thus divergent between species.

The immune-related IFITM proteins (IFITM1, IFITM2, and IFITM3 in humans) may represent the earliest acting restriction factors yet identified. The *IFITM* family also includes the *IFITM5* and *IFITM10* genes with no known immune function [3]. *IFITM* genes are present among a wide range of vertebrate animal species, and they may have originated in early unicellular eukaryotes via horizontal gene transmission from a bacterium [4]. Since then, expansions within genomes have given rise to unique *IFITM* gene repertoires that vary at the level of sequence and copy number. To date, all immune-related IFITM proteins identified in animals (metazoans) display antiviral function [5–7]. Even *IFITM*-like genes in *Mycobacteria* inhibit virus infection when expressed in human cells [8].

As residents of membranes at the interior and exterior of the cell, they block the entry step of diverse viruses [9,10] by inhibiting virus–cell fusion. The mechanisms behind this protection involve altering the biophysical properties [11–13] or cholesterol content [14] of the cellular membranes in which they are found. These proteins inhibit many enveloped viruses, including influenza A virus (IAV), West Nile virus, dengue virus, severe acute respiratory syndrome coronavirus, hepatitis C virus, and Ebola virus [15], as well as lentiviruses including HIV-1 and SIV [16–18]. While the majority of studies have relied on *in vitro* infection systems, it is well established that IFITM3 restricts virus infection *in vivo*.

1 Virus & Immunity Unit, Institut Pasteur, Paris, France
2 Department of Microbial Infection & Immunity, The Ohio State University, Columbus, OH, USA
3 Lady Davis Institute, McGill University, Montreal, QC, Canada
4 CNRS-URA 3015, Paris, France
5 Vaccine Research Institute, Creteil, France
   *Corresponding author. Tel: +33 1456 88576; E-mail: alex.compton@pasteur.fr
   **Corresponding author. Tel: +33 1456 88353; E-mail: schwartz@pasteur.fr

Ifitm3-deficient mice fail to clear infection by otherwise mild strains of IAV [19,20].

Using a cellular coculture system, we and others identified new antiviral functions of IFITM proteins during HIV-1 infection [21–23]. We showed that IFITM proteins, in particular IFITM3, block the spread of HIV-1 from infected to uninfected T cells. Surprisingly, this function was primarily the result of interactions occurring between IFITM3 and virus in the infected cells. We found that IFITM3 in the virus-producing cell decreases virion infectivity at the level of virus–cell fusion and that IFITM3 becomes incorporated into nascent virions. This mechanism of antiviral function may apply to other lentiviruses as well as diverse families of enveloped viruses. Therefore, IFITM proteins are restriction factors of increasingly broad scope.

While human IFITM3 is described as a resident of endosomal and lysosomal membranes [24], we observed that a portion of IFITM3 is detectable at the surface of transfected 293T cells and in primary CD4$^+$ T cells [21]. In fact, IFITM3 can be observed at many different subcellular compartments and its localization is regulated by various post-translational modifications [25]. The fate of IFITM3 is governed by phosphorylation [16,26], ubiquitination [27], palmitoylation [27,28], and methylation [29]. These regulatory processes impact the localization and turnover of IFITM3 in the cell, and as a result, they are critical to its antiviral function. During biosynthesis, IFITM3 protein is trafficked to the plasma membrane and endocytosed. This latter step is driven by an internalization motif (YxxΦ, YEML in human IFITM3) that is recognized by the µB unit of the AP-2 complex, resulting in the sorting of IFITM3 into late endosomes, multivesicular bodies, and lysosomes [26,30]. Furthermore, an overlapping motif (PPxY, PPNY in human IFITM3) recruits the E3 ubiquitin ligase NEDD4 to promote IFITM3 ubiquitination and turnover via lysosomes [31]. Phosphorylation of tyrosine residue 20 (Y20) common to the two motifs inhibits both endocytosis and ubiquitination, causing an accumulation of IFITM3 and redistribution to the plasma membrane [26]. Mutation or deletion of Y20 produces a similar effect [30]. Interestingly, a single nucleotide polymorphism (SNP) (rs12252-C) in human *IFITM3* is predicted to produce an alternatively spliced transcript that encodes a protein lacking these two regulatory motifs. This putative truncated form of IFITM3 (Δ1–21) is largely confined to the plasma membrane when expressed in cell lines [16]. Intriguingly, rs12252-C is associated with severe outcomes following IAV infection [20,32–34]. These epidemiologic studies coincide with *in vitro* experiments showing that IFITM3 Δ1–21 fails to accumulate in the endosomal compartment, where IAV undergoes pH-dependent fusion to access the cytoplasm. However, endogenous expression of the putative truncated form of human IFITM3 has not been demonstrated to date. While these previous reports reveal how synthetic mutations in IFITM3 affect the restriction of RNA viruses such as IAV and vesicular stomatitis virus (VSV), it remains unclear how they may regulate the activity against other viruses with different cell entry strategies. Furthermore, very little is known about natural, genome-encoded mutations that may affect IFITM function in diverse animal species.

HIV-1 is believed to carry out the initial (fusion) and terminal (budding) steps of its life cycle at the plasma membrane of T lymphocytes [35]. Given that the amount of IFITM3 at the cell surface most likely dictates its ability to restrict HIV-1 entry and the infectivity of nascent budding virions, we hypothesized that post-translational modifications affecting cell surface association will impact the activity of IFITM3 against HIV-1. Here, we report that endocytosis and ubiquitination are negative regulators of IFITM3 anti-HIV activity. Furthermore, we show that post-translational regulation of IFITM3 may result in a functional trade-off: alterations that improve the function against one virus can inhibit its activity against other viruses. As a testament to their functional importance, periodic diversification of residues within the two regulatory motifs of IFITM3 is observed during primate evolution, resulting in variants with different potency and specificity. Finally, our multifaceted analysis has allowed us to retrace the origins of *IFITM* in primates and provides an explanation for the recurrent gene duplication observed in this antiviral gene family.

Results

Mutation in IFITM3 alters subcellular localization and anti-HIV activity

IFITM3 contains two hydrophobic domains conserved in other IFITM family members, but is divergent in its amino- and carboxy-termini. The amino-terminal sequence motifs recognized by NEDD4 and the AP-2 complex are adjacent and overlap at the tyrosine at residue 20, found just upstream of an internal methionine (which serves as the translation start site in IFITM1 and the Δ1–21 construct of IFITM3) [25] (Fig 1A).

293T cells were selected as a suitable system to study the impact of post-translational modifications on IFITM3 function because they express very low levels of constitutive IFITM3. Transfection of FLAG-tagged IFITM3 into 293T results in expression levels comparable to, but less uniform than, those induced by type-I interferon (Fig EV1A) and localization to disperse intracellular vesicles and the plasma membrane (Fig 1B). As previously described [16], the subcellular localization of the Δ1–21 variant is mostly restricted to the plasma membrane (Fig 1B). A mutant deficient in cysteine residues (referred to as Δpalm because it prevents palmitoylation of IFITM3 [27]) results in a predominantly perinuclear localization with additional diffuse staining throughout the cytoplasm. Western blot and flow cytometric analysis reveal quantitative differences in protein expression. Levels of the Δ1–21 variant are elevated relative to full-length protein, while Δpalm is expressed at lower levels (Fig 1C and D).

To address how mutation in IFITM3 affects its activity against HIV-1, virus was produced in 293T cells via co-transfection with the HIV-1 molecular clone pNL4-3, pVpr-Blam (which allows the detection of virion access into the cytoplasm), and plasmids expressing IFITM3 mutants (as performed in [21]). Consistent with its enhanced localization to the cell surface, which also serves as the site for virus assembly and budding, the Δ1–21 variant exhibits increased levels of virion incorporation relative to full-length IFITM3 (Fig 1E). Importantly, viruses produced in the presence of the Δ1–21 variant are further reduced in virion infectivity when incubated with fresh SupT1 T-cell targets, as evidenced by reduced virus–cell fusion at 4 h (Fig 1F) and reduced productive viral infection at 48 h (Fig 1G). Virus produced in the presence of MxA was used as an additional negative control. Confocal immunofluorescence microscopy confirms that surface-associated IFITM3 can be localized to sites of HIV-1 budding tagged by the presence of mature
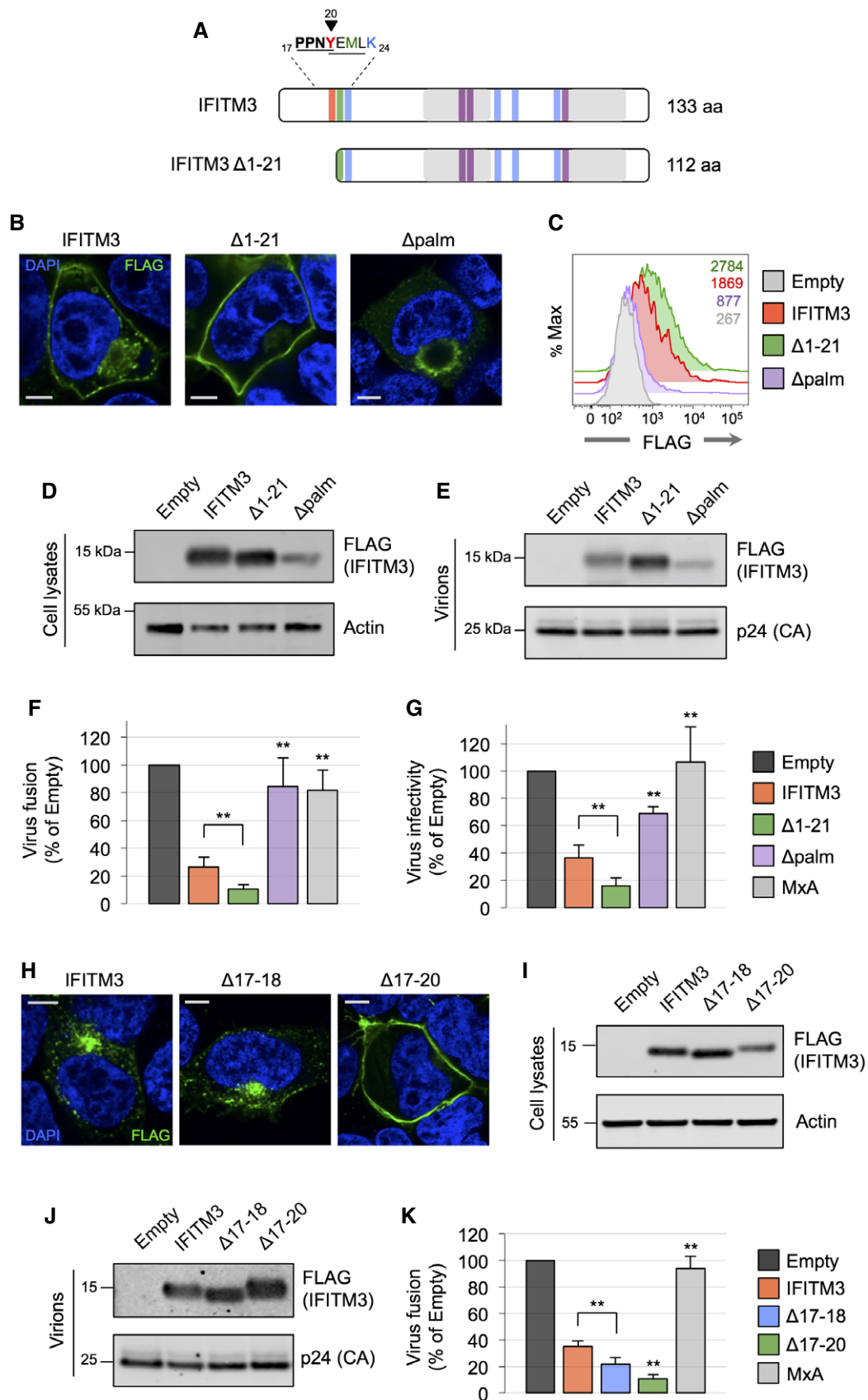
Figure 1.

Figure 1. Mutation in IFITM3 alters protein subcellular localization and anti-HIV activity.

A   A schematic of the IFITM3 protein is shown, with gray boxes indicating transmembrane domains and colored bars indicating residues targeted for post-translational modification: ubiquitinated lysines (blue), palmitoylated cysteines (purple), and a phosphorylated tyrosine (red). Residues 17–24 are shown in detail to highlight two adjacent, overlapping motifs that recruit NEDD4 (PPNY) and the AP-2 complex (YEML). The IFITM3 Δ1–21 variant initiates translation at an internal methionine residue (green) and thus lacks these motifs.

B   Confocal fluorescence microscopy of 293T cells transfected with 0.5 μg pQCXIP encoding IFITM3 variants containing N-terminal FLAG (pQCXIP-FLAG-IFITM3) and immunostained with anti-FLAG M2 antibody. Scale bar, 5 μm.

C   Flow cytometric analysis of transfected cells in (B) immunostained with anti-FLAG M2 antibody. Corresponding mean fluorescence intensity values are shown.

D   SDS–PAGE of cell lysates derived from 293T cells transfected in (B) followed by immunoblotting with anti-FLAG M2 and anti-actin antibodies.

E   SDS–PAGE of OptiPrep-purified supernatants (25 ng p24 equivalent) derived from 293T cells transfected with pQCXIP-FLAG-IFITM3 variants, HIV-1 pNL4-3, and Vpr-Blam plasmid followed by immunoblotting with anti-FLAG M2 and anti-p24 Gag (183-H12-5C).

F   OptiPrep-purified supernatants from (E) were incubated with SupT1 target cells for 4 h and virus–cell fusion was scored by flow cytometry. Mean + SD of 5–10 experiments (each performed with virus produced from an independent transfection) is shown.

G   Viruses used in (E) were used to infect SupT1 cells and productive infection was scored at 48–60 h by immunostaining with the KC57 antibody and flow cytometry. Expression of pCMV-MxA served as a negative control. The mean + SD of 5–10 experiments is shown.

H   Confocal fluorescence microscopy of 293T cells transfected with 0.5 μg pQCXIP-FLAG-IFITM3 variants and immunostained with anti-FLAG M2 antibody.

I   SDS–PAGE of cell lysates derived from 293T cells transfected in (H) followed by immunoblotting with anti-FLAG M2 and anti-actin antibodies. Scale bar, 5 μm.

J   SDS–PAGE of OptiPrep-purified supernatants (25 ng p24 equivalent) derived from 293T cells transfected with pQCXIP-FLAG-IFITM3 constructs, HIV-1 pNL4-3, and Vpr-Blam plasmid followed by immunoblotting with anti-FLAG M2 and anti-p24 Gag.

K   OptiPrep-purified supernatants from (J) were incubated with SupT1 target cells for 4 h and virus–cell fusion was scored by flow cytometry. The mean + SD of three experiments is shown.

Data information: Western blot and microscopy images are representative of three independent experiments. Unpaired *t*-test (two-sided), **$P < 0.005$. Statistical comparisons were made between the condition indicated and IFITM3 WT. Normality was determined by the KS test and variance determined by the *F*-test.

Gag protein (Fig EV1B). Results with an IFITM3 mutant encoding a single residue deletion at position 20 (ΔY20) reproduced those of Δ1–21, strongly suggesting that the tyrosine residue and the two overlapping regulatory motifs to which it belongs are crucial to the enhancement of anti-HIV activity observed (Fig EV1C–E). Thus, the extent of inhibition of HIV-1 infectivity is associated with cell surface localization and the increased detection of IFITM3 in virions. We previously demonstrated that IFITM1, which naturally lacks the amino-terminus present in IFITM3, only modestly restricts HIV-1 infectivity [21]. Thus, the absence of an amino-terminus *per se* is not sufficient to enhance anti-HIV-1 activity. Rather, IFITM3 contains other intrinsic determinants that enable a potent HIV-1 restriction that can be amplified by the removal of its amino-terminus.

To assess the involvement of distinct regulatory activities in the regulation of IFITM3 activity, we took advantage of additional IFITM3 mutants in which the NEDD4-binding site alone (Δ17–18) or both the NEDD4- and the AP-2-binding sites (Δ17–20) are disrupted. Immunofluorescence microscopy confirmed previously published results [16] showing that Δ17–20 is enriched at the cell surface (Fig 1H). Similar to Δ1–21, the Δ17–18 mutant exhibits slightly elevated protein levels relative to full-length IFITM3. Importantly, the Δ17–20 variant does not share this feature, and it is even expressed at lower levels relative to full-length IFITM3 (Figs 1I and EV1F). Both the Δ17–18 and Δ17–20 variants display an increased propensity for virion incorporation, with the mutant in which endocytosis is disrupted (Δ17–20) showing the greatest phenotype (Fig 1J). Consistently, the Δ17–20 variant demonstrates the most profound inhibition of HIV-1 particle fusogenicity (Fig 1K) and infectivity (Fig EV1G). Therefore, the enhancement of IFITM3 antiviral activity is associated with its subcellular localization and is not solely dependent on protein levels. When we employed a L23Q mutant to inhibit protein endocytosis [26] without disturbing the NEDD4-binding motif, we found that this single amino acid change also results in more pronounced restriction of HIV-1 infectivity relative to wild-type IFITM3 (Fig EV1H and I). These results collectively suggest that motifs interacting with endogenous NEDD4 and AP-2 act in an additive fashion to negatively regulate the anti-HIV activity of IFITM3.

The E3 ubiquitin ligase NEDD4 regulates the activity of IFITM3 against HIV-1

We directly tested the regulatory effect of NEDD4 in virus-producing cells using a system in which NEDD4 is co-expressed by transfection with IFITM3 or the Δ1–21 variant in 293T cells. The co-expression of NEDD4 resulted in lower levels of IFITM3 in cell lysates, an effect that was not observed for the catalytically inactive NEDD4 mutant C867A (Fig EV2A). These results confirm that NEDD4-mediated ubiquitination accelerates the turnover of IFITM3 [31]. Moreover, NEDD4 co-expression diminished the levels of IFITM3 incorporated into HIV-1 virions (Fig EV2A). In contrast to its typical expression pattern in the cytoplasm and on the cell surface, confocal immunofluorescence microscopy revealed that IFITM3 becomes mostly intracellular in cells co-expressing NEDD4, but not in those with inactive NEDD4 C867A (Fig EV2B and C). NEDD4 induced the accumulation of IFITM3 in large vesicular compartments that partially colocalize with LAMP1 (Fig EV2D). In contrast, protein levels of the Δ1–21 variant in cell lysates or in virions were unaffected by NEDD4, and the localization remained predominantly cell surface oriented (Fig EV3D). Collectively, these findings suggest that NEDD4 regulates IFITM3 levels in cells producing HIV-1 and thus may regulate its antiviral effect. They also highlight how variants of IFITM3 missing key elements of the amino-terminus may confer escape from NEDD4 and lead to enhanced antiviral function in the cell.

The amino-terminus of IFITM3 regulates activity against HIV-1 in T cells

To study the regulation of IFITM3 protein in the natural target cells of HIV-1, we took advantage of T-lymphocyte cell lines (SupT1)
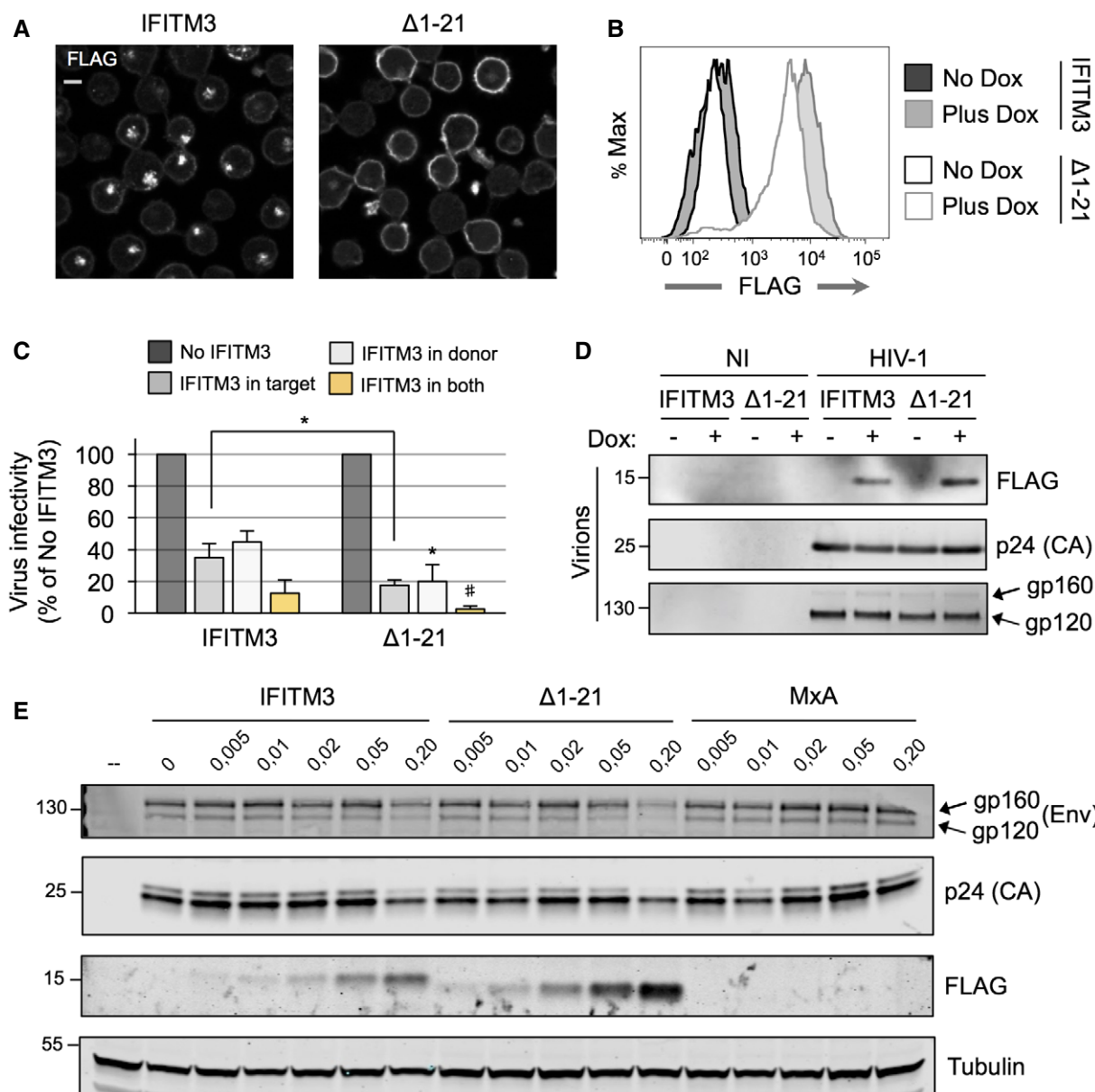
Figure 2. Mutation of N-terminal regulatory motifs of IFITM3 in T cells enhances the restriction of HIV-1.

A Confocal fluorescence microscopy of SupT1 T cells transduced with Tet-inducible pQCXIP-FLAG-IFITM3 or pQCXIP-FLAG-IFITM3 Δ1–21 (Tet-ON) immunostained with anti-FLAG M2 antibody following overnight treatment with 500 ng/ml doxycycline. Scale bar, 10 μm.

B Tet-ON SupT1 cell lines were treated or not with 500 ng/ml doxycycline overnight and induction of IFITM3 protein was assessed by anti-FLAG M2 immunostaining and flow cytometry.

C Tet-ON SupT1 cell lines were productively infected with NL4-3 VSV-G and then treated with 500 ng/ml doxycycline overnight to produce virus from IFITM3⁻ and IFITM3⁺ cells; 25 ng p24 equivalents of purified supernatants was used to infect fresh Tet-ON SupT1 cells, which were previously treated with 500 ng/ml doxycycline or not. Infection was scored at 72 h postinfection by immunostaining with KC57 and flow cytometry. Mean + SD of three experiments is shown.

D About 25 ng p24 equivalents of virus used in (C) was subjected to SDS–PAGE. Immunoblotting was performed using anti-FLAG M2, anti-p24 Gag, and anti-gp120 Env (NIH #288) antibodies.

E 293T cells were transfected with the indicated amount of pQCXIP-FLAG-IFITM3 or pQCXIP-FLAG-Δ1–21 or pCMV-MxA and 1.0 μg of HIV-1 pNL4-3. SDS–PAGE was performed on whole-cell lysates followed by immunoblotting with anti-FLAG M2, anti-p24 Gag, anti-Env gp120 (NIH #288), and anti-tubulin antibodies.

Data information: Western blot and microscopy images are representative of three independent experiments. Unpaired *t*-test, *$P < 0.05$, ‡$P = 0.12$, nonstatistically significant. Comparisons were made between the condition indicated and the corresponding condition in Tet-ON IFITM3 cells.

engineered to allow for Dox-inducible expression of IFITM3 protein variants [17,21]. Following Dox treatment of these cells, expression levels are uniform and full-length IFITM3 localizes mostly to the cell interior, while the Δ1–21 variant is predominantly found at the surface (Fig 2A), mirroring the results in 293T cells. Importantly, we observed the induction of higher levels of full-length IFITM3

compared to the Δ1–21 variant in its respective cell line (Fig 2B). Using this T cell-based system, we tested the relative antiviral potential of IFITM3 in both donor and target cells. We produced virus in the presence or absence of IFITM3 variants and subsequently infected target T cells in which IFITM3 variants were induced or not. As previously reported [21], IFITM3 restricts HIV-1 infection within donor and target cells in an additive fashion (Fig 2C). However, the Δ1–21 variant exhibits superior antiviral activity at both stages, such that infection is almost completely blocked when it is present in both donor and target cells (Fig 2C). These data demonstrate that removal of the amino-terminus enhances both antiviral functions fulfilled by IFITM3 during HIV-1 infection. Despite the relatively lower level of protein induction in this system, and in agreement with its localization at the cell surface, the Δ1–21 variant is enriched in virions (Fig 2D). Importantly, we did not detect IFITM3 in supernatants from noninfected cells, strongly suggesting that the majority of signal detected originates from within virus particles [21] (Fig 2D). Nonetheless, because IFITM proteins can also be found in exocytic vesicles [36], we performed density gradient purification of virions produced in the presence of full-length IFITM3 and the Δ1–21 variant. As previously reported [21], full-length IFITM3 co-sediments with HIV-1 Gag protein and is nearly absent from fractions containing lower-density microvesicles, and the pattern was similar for Δ1–21 (Fig EV3).

A recent publication reported that IFITM3 antagonizes HIV-1 envelope protein, altering both the maturation of gp120 and inhibiting its incorporation into virions produced in 293T cells [23]. However, and consistent with our previous publication [21], the induction of IFITM3 or the Δ1–21 variant did not affect gp120 levels in virions produced in T-cell lines (Fig 2D). To explore further the effect of IFITM3 on HIV-1 Env in virus-producing cells, we co-transfected 293T cells with HIV-1 pNL4-3 and titrating amounts of plasmid encoding IFITM3, the Δ1–21 variant, or MxA. We observed that gp120 levels were slightly reduced only at the highest level of IFITM3 overexpression (Fig 2E). The Δ1–21 variant reduced gp120 levels somewhat further in a manner consistent with its elevated expression, while MxA overexpression had no effect. Interestingly, we also found that reduction in gp120 was accompanied by a concomitant decrease in HIV-1 p24 levels, possibly suggestive of a global effect on virus translation (Fig 2E). Therefore, while IFITM3-mediated restriction of HIV-1 infectivity may involve Env antagonism, this effect is cell type dependent and expression level dependent. We propose that the mechanistic basis for IFITM3 antiviral function against HIV-1 lies primarily with its cell surface localization, which is associated with its incorporation into virions budding from the same compartment.

Recurrent duplication and divergence of primate *IFITM3* over evolutionary time

Given our finding that synthetic mutants in the amino-terminus of IFITM3 exhibit enhanced anti-HIV-1 activity, we chose to examine the functional consequences of standing variation in *IFITM3* genes from nonhuman primates. Dozens of species harbor simian immunodeficiency virus (SIV) strains in the wild, infections that have likely persisted for millions of years in coevolution with their hosts [2]. Experimental approaches combining *in silico* genomic analysis and *in vitro* or *in vivo* infection assays have revealed that primate

immunity genes, such as *APOBEC3G*, *TRIM5*, *tetherin*, and *SAMHD1*, are undergoing adaptive evolution in ways that impact lentiviral infections [37]. Our results prompted us to ask whether the antiviral function and specificity of IFITM3 may also be dynamic and subject to natural selection on evolutionary timescales.

Some previous reports focusing on the evolution of the *IFITM* gene family in vertebrates have shown that, compared to the five *IFITM* genes present on human chromosome 11, the number of *IFITM* genes per species may vary as a result of gene duplication events [4,38]. To build a comprehensive understanding of *IFITM* evolution in primates, we used comparative genomics to identify *IFITM* genes from full reference genomes. Aided by the Genomicus toolkit [39] and the Ensembl gene database (www.ensembl.org), we characterized the *IFITM* locus in simian and prosimian primate species. Simians consist of haplorhine primates, including hominoids (humans, chimpanzee, gorilla, orangutan, and gibbon), Old World Monkeys [rhesus macaque, olive baboon, and vervet monkey (African Green Monkey)], and New World Monkeys (common marmoset), while prosimians consist of strepsirrhine primates (mouse lemur and bushbaby) as well as a Tarsiiforme relict species (tarsier). This analysis yielded several novel insights into *IFITM* evolution. First, the "canonical" *IFITM* gene locus found in humans is atypical with regard to gene number and gene composition. For example, the *IFITM* locus of the prosimian bushbaby species is syntenic with that of humans, but it does not contain *IFITM1* or *IFITM2*. Instead, it contains two adjacent copies of *IFITM3* resulting from gene duplication (a third copy of *IFITM3*, also the product of gene duplication, is located on a separate chromosome) (Fig 3A). In fact, while the last common primate ancestor (LCPA) is predicted to contain only three *IFITM* genes, primate evolution is punctuated by *IFITM* gene gain and gene loss events (Fig 3B). Many of the modern primate genomes analyzed show evidence of *IFITM3* gene duplication, while the tarsier contains only a single *IFITM* gene, and it is *IFITM3* (Fig 3B). The number of *IFITM3* genes listed for each species is a minimal estimate, as we only considered *IFITM3* sequences predicted to be protein coding by Ensembl (sequences containing an intact open reading frame and lacking premature stop codons). These data suggest that *IFITM3* is the oldest of the *IFITM* family members with known antiviral activities. Furthermore, the genomes of hominoids (apes) revealed that *IFITM2* is a relatively recent genetic innovation specific to humans, chimpanzee, and gorilla (Fig 3B). Overall, the evolutionary trajectory of *IFITM* in primates suggests a recurrent need for functional diversification.

We used BLAST analysis to confirm the identity of sequences in Ensembl and also to supplement our *IFITM3* sequence list with additional species (such as an additional strepsirrhine species (the sifaka) and an Old World Monkey of the *Colobinae* subfamily, the colobus monkey). From these combined analyses, we compiled an alignment of *IFITM3* coding sequences and performed phylogenetic reconstructions (Fig 4A and B, and Appendix Fig S1). Notably, our analysis uncovered recurrent mutation in the amino-terminus of primate *IFITM3*, including many examples found in the motifs controlling ubiquitination and endocytosis (selected examples shown in Fig 4A). *IFITM3* sequences from prosimians demonstrate that these motifs were likely intact in the common ancestor of all primate species (Fig 4A). However, each one of the strepsirrhine species contains two *IFITM3* genes in their respective *IFITM* locus,
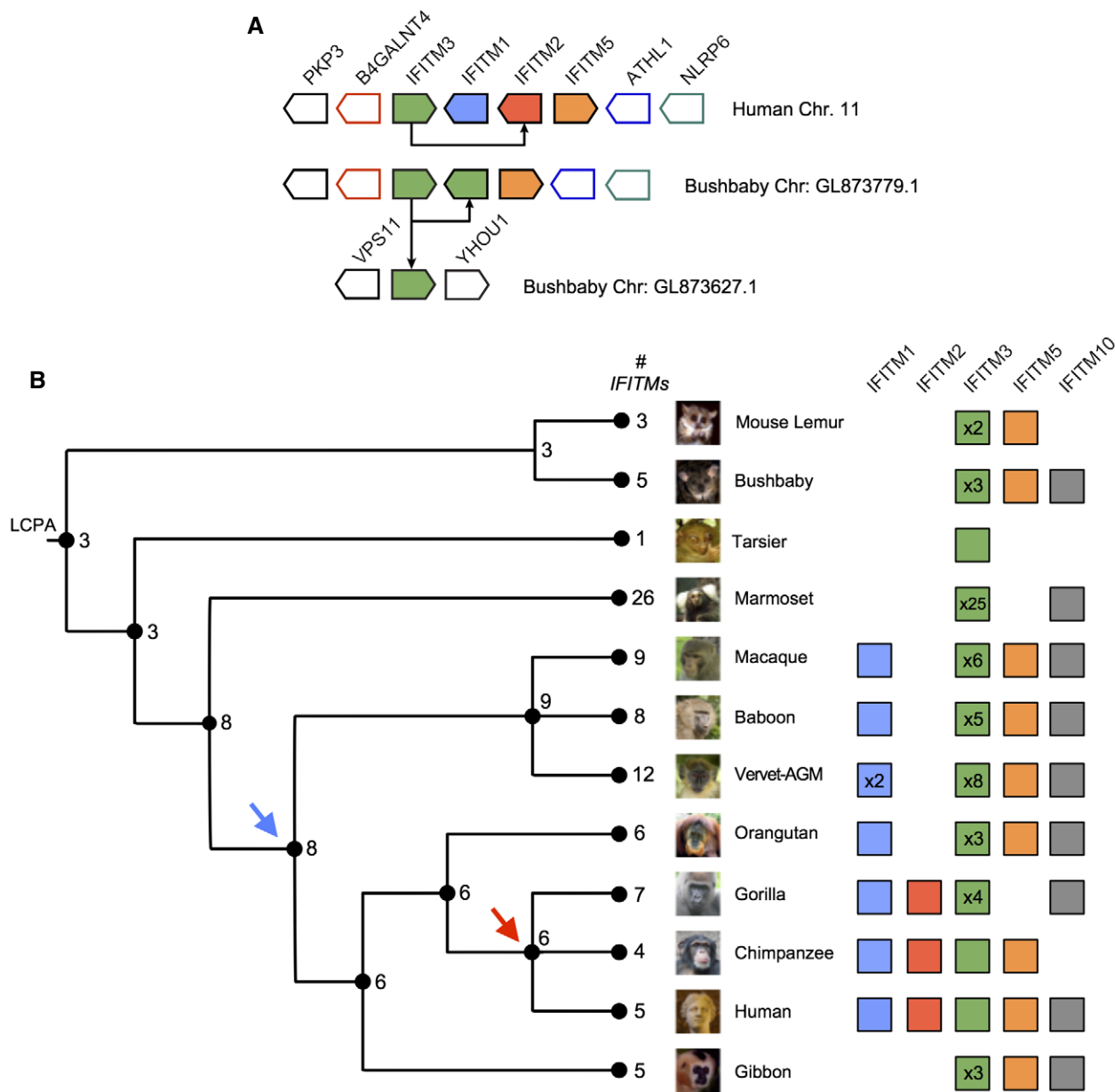
Figure 3.   Retracing the origins of *IFITM* in primates.

A   A comparison of the *IFITM* locus on chromosome 11 of the human reference genome (GRCh38.p5) and the corresponding locus in the bushbaby reference genome (OtoGar3) visualized using Genomicus v84.01. Synteny is observed between human *IFITM* and bushbaby *IFITM*, as evidenced by the conserved flanking genes *B4GALNT4* and *ATHL1*. The bushbaby locus lacks *IFITM2* and *IFITM1* genes. In addition, it contains two adjacent *IFITM3* genes, as well as a third *IFITM3* gene located in a different genomic context, indicative of gene duplication events.

B   A gene gain/loss tree summarizing the phylogenetic history of the *IFITM* gene family in primates, using annotated reference genomes in Ensembl. The number at a branch tip refers to the number of *IFITM* genes present in a given extant species, while the number at each node refers to the number present in an ancestral species. Differences in gene number at tips and nodes represent significant gene gain events (expansions) or gene loss events (contractions) based on a *P*-value calculation of < 0.01 determined by CAFE (Computational Analysis of gene Family Evolution) [55]. The makeup of the *IFITM* repertoire for each species, as determined by comparative genomics and the *IFITM* gene family tree in Ensembl, is detailed to the right. When multiple copies of *IFITM* genes were identified, the total number is listed inside the box. The gene numbers estimated for the mouse lemur and bushbaby in Ensembl were adjusted following phylogenetic analysis of *IFITM* homologs in Genomicus as well as BLAST searches of the NCBI GenBank database. Blue and red arrows indicate the emergence of *IFITM1* and *IFITM2* genes, respectively.

and one copy of each pair contains mutations that disrupt motifs for ubiquitination and/or endocytosis. This finding suggests that a tandem duo of *IFITM3* genes with potentially divergent functional properties has evolved independently on multiple occasions.

Meanwhile, similar observations were made in simian species. It was previously recognized that the marmoset monkey genome contains dozens of *IFITM3* sequences in its genome [38]. Interestingly, the array of 25 *IFITM3* variants present in this species carry
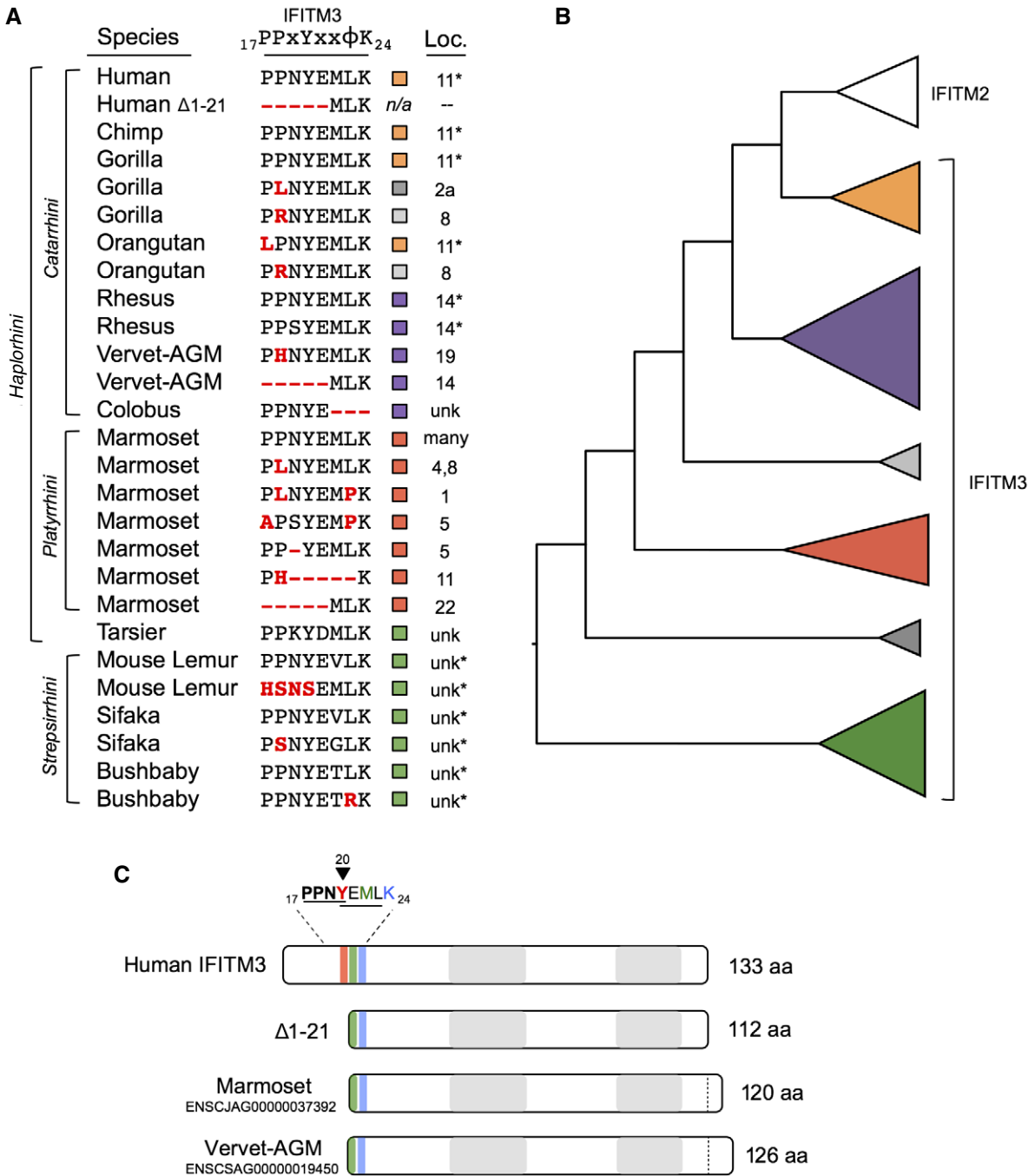
Figure 4.　Recurrent duplication and divergence of primate *IFITM3* over evolutionary time.

A　A partial protein alignment of select *IFITM3* genes from various primate species for which a reference genome is available and accessible in Genomicus. Sequences from the mouse lemur and colobus monkey were identified by BLAST analysis of reference genomes in NCBI GenBank. Gene location is indicated, when available, by chromosome number, and an asterisk indicates that the given gene sequence falls into a canonical *IFITM* locus with flanking *B4GALNT4* and *ATHL1* genes. The suborder and parvorder (from left to right) indicate taxonomical relationships between species. Residues bolded in red highlight nonsynonymous substitutions that disrupt canonical motifs for the recruitment of NEDD4 and AP-2. A complete protein alignment of all *IFITM* sequences analyzed in this study is available in Appendix.

B　A phylogenetic gene tree (cladogram) indicates the relationship among *IFITM3* sequences analyzed in this study. The final consensus tree was made by merging results from neighbor joining and maximum-likelihood phylogenetic reconstructions using both nucleotide and amino acid sequences in Ensembl (see Fig EV4 for robustness measurement by Bayesian inference). Branch lengths are normalized and arbitrary. The size of triangles at the tree tips roughly corresponds to the number of sequences contained therein. Note that the *IFITM2* gene is the most recent member of the *IFITM* locus, appearing only in humans, chimpanzee, and gorilla genomes.

C　A graphical representation of naturally occurring truncated forms of *IFITM3* identified in the vervet and marmoset reference genomes, as compared to the putative Δ1–21 variant in humans.

many iterations of mutations or deletions that disrupt the motifs necessary for interaction with NEDD4 and/or AP-2 (Fig 4A and Appendix Fig S1).

These cases of *IFITM3* duplication and divergence were not isolated to far-removed primate species, since we also found similar patterns in the catarrhine parvorder to which humans belong. We identified a single *IFITM3* sequence in the colobus monkey that contains a deletion (Δ22–24) eliminating the motif necessary for AP-2-mediated endocytosis as well as a neighboring lysine residue (K24) targeted for ubiquitination [27] (Fig 4A). Furthermore, codons 17 and 18 of *IFITM3*, corresponding to the critical proline residues necessary for its interaction with and ubiquitination by NEDD4 [31], have diversified in *IFITM3* genes in the vervet, gorilla, and orangutan. This latter species contains an *IFITM3* that is syntenic with human *IFITM3* on chromosome 11 and contains a P17L mutation. Phylogenetic analysis of primate *IFITM3* showed branching patterns that reproduce major taxonomic groups, with a few exceptions (Figs 4B and EV4A). While *IFITM3* from prosimians clearly represents the basal clade, some *IFITM3* sequences found in gorilla, vervet, and orangutan genomes form two outlier branches (in gray). These sequences appear to predate other *IFITM3* sequences found in the same species, suggesting that they most likely represent duplication events that took place in simian ancestors. Importantly, the maintenance of these sequences in multiple species until present day may indicate that they retain functional importance (Figs 4B and EV4A).

Since we found that many naturally occurring mutations identified in primate *IFITM3* effectively mimic the synthetic mutants tested in this study, we predicted that they might similarly confer escape from the cellular processes of ubiquitination and/or endocytosis. A further observation that is especially pertinent to the data shown in this study is that certain *IFITM3* sequences identified in the vervet and marmoset genome closely resemble the human Δ1–21 construct, with each lacking the amino-terminus and initiating translation at an internal methionine (Fig 4C). In addition, we observed a few *IFITM3* sequences in which the initial methionine is absent or mutated (Appendix Fig S1), which could also give rise to truncated IFITM3 proteins similar to the Δ1–21 construct.

Naturally occurring mutations in IFITM3 disrupt regulatory motifs and toggle antiviral activity

We next characterized the functional consequences of select nonhuman IFITM3 mutations by introducing them into the human IFITM3 background. Transfection into 293T cells and confocal immunofluorescence microscopy showed that Δ22–24 resulted in a shift to the cell surface (Fig 5A). Predominant plasma membrane staining was also observed for marmoset-specific IFITM3 mutations, reiterating an effect on protein endocytosis through ablation of the AP-2-recruiting motif (Fig 5A). As expected, primate mutations in the NEDD4-binding motif (P17L found in orangutan and P18H found in vervet) did not grossly affect the subcellular localization of IFITM3. To assess the extent to which each variant could be ubiquitinated in cells, we immunoprecipitated IFITM3 from cells co-expressing NEDD4 or catalytically inactive NEDD4 C867A. In agreement with a previous report [31], ubiquitinated forms of human full-length IFITM3 can be detected following the overexpression of NEDD4, while the Δ1–21 variant (which lacks the NEDD4-binding motif)

was less ubiquitinated (Fig 5B). The P17L and P18H mutations also led to lower levels of ubiquitination, especially pools modified with two or three ubiquitin moieties (as indicated by ** and ***, respectively). The IFITM3-specific antibody used here recognized all but the Δ22–24 variant. We confirmed the presence of ubiquitin using an antibody capable of recognizing mono- and polyubiquitinated proteins (Fig 5B, colored image). The direct labeling of ubiquitin showed that the Δ22–24 variant is modified by NEDD4 to an intermediate extent, since it contains an intact NEDD4-binding site yet lacks one nearby lysine residue. Ubiquitination was also detected in the presence of catalytically inactive NEDD4 C867A, albeit at lower levels (Fig 5B). These results reveal that the natural P17L, P18H, and Δ22–24 mutations prevent normal protein ubiquitination not only by ectopic NEDD4, but also by endogenous E3 ligases in 293T cells. Examination of whole-cell lysate fractions confirmed the expression of all IFITM3 variants (Fig 5C). In accordance with the degree of ubiquitination observed in the immunoprecipitated fractions, certain NEDD4-sensitive variants of IFITM3 were detected at lower levels (relative to the inactive NEDD4 C867A control). Notably, these naturally occurring mutations that disrupt subcellular localization (Fig 5A) and/or diminish NEDD4-mediated ubiquitination (Fig 5B) also exhibit enhanced restriction of HIV-1 virion infectivity relative to full-length human IFITM3 (Fig 5D).

We previously showed that IFITM3 performs two antiviral roles in the setting of HIV-1 infection: (i) inhibition of virus particle infectivity within infected cells (donor cell effect) and (ii) protection of uninfected cells from incoming cell-free virus particles (target cell effect) [21]. To measure the functional impact of IFITM3 variation in both of its antiviral roles, we tested the ability of primate IFITM3 variants to inhibit HIV-1 entry when expressed in uninfected target cells. To this end, we achieved the stable expression of IFITM3 variants in 293T cells transduced with CD4 and CXCR4 (293T 4 × 4 cells) [40] and tested their relative resistance to infection by HIV-1. Importantly, we achieved similar levels of protein expression across all conditions (Fig EV5A), and the differential subcellular localization displayed between IFITM3 variants was maintained (Fig EV5B). When these cells were challenged with HIV-1, synthetic and natural IFITM3 variants containing amino-terminus mutations conferred elevated resistance to incoming HIV-1 relative to human IFITM3 (Fig 5E). The greatest degree of virus restriction was achieved by mutants with the enhanced surface localization (ΔY20, Δ1–21, and Δ22–24).

Since synthetic mutations in IFITM3 that affect regulation by NEDD4 and the AP-2 complex have previously been shown to alter sensitivity to RNA viruses such as IAV and VSV, we also examined the extent of IAV entry restriction in the same 293T 4 × 4 cell lines. In line with previous findings [9], we confirmed that IFITM3 is a more potent inhibitor of IAV compared to IFITM1 and IFITM2 (Fig EV5C). While human IFITM3 restricts IAV infection by nearly 50-fold, ΔY20 and the Δ1–21 variant are markedly less active (Fig 5F), consistent with previous studies [20]. Furthermore, while IFITM3 carrying the P17L and P18H mutations retained the potent restriction of IAV, the Δ22–24 deletion specific to colobus monkey IFITM3 reduces anti-IAV activity by approximately 20-fold (Fig 5G). We also tested the antiviral activity of a full-length "native" colobus IFITM3 protein, which encodes all amino acid substitutions that differ from human IFITM3 (Appendix Fig S1), and the results were similar (Fig 5G). These findings suggest that the functionally informative
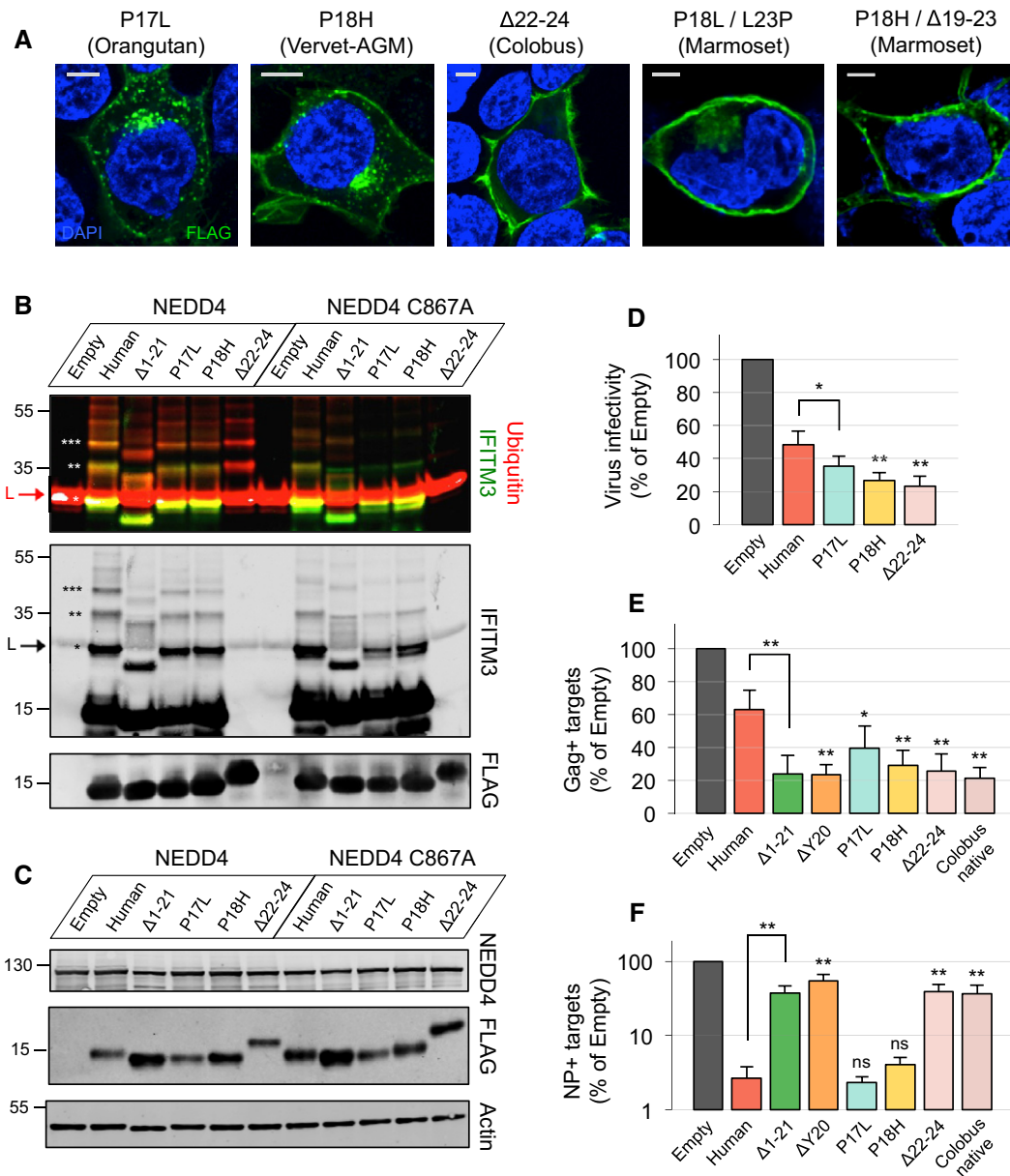
Figure 5. Natural mutations in *IFITM3* disrupt regulatory motifs and toggle antiviral activity.

A   Confocal fluorescence microscopy of 293T cells transfected with 0.5 µg of pQCXIP-FLAG-IFITM3 mutated at the indicated residues and immunostained with anti-FLAG M2 antibody. Scale bars, 5 µm. The P17L, P18H, Δ22–24, P18L/L23P, and P18H/Δ19–23 mutations were introduced into the human IFITM3 background.

B   SDS–PAGE of FLAG-immunoprecipitated fractions from 293T cells following transfection of 0.5 µg of pQCXIP-FLAG-IFITM3 variants and 0.5 µg of pCI-HA-NEDD4 or pCI-HA-NEDD4 C867A. Immunoblotting was performed with anti-FLAG M2, anti-IFITM3 (Abcam, EPR5242), and an anti-ubiquitin antibody (Enzo Life Sciences, recognizing K^{29}-, K^{48}-, and K^{63}-linked mono- and polyubiquitinylated proteins). "L" indicates the presence of light chain antibody derived from the FLAG antibody-coupled beads used for immunoprecipitation. *, **, and *** indicate mono-, di-, and triubiquitinated forms of IFITM3.

C   SDS–PAGE of whole-cell lysate input fractions from 293T cells used in (B). Immunoblotting was performed with anti-FLAG M2, anti-NEDD4, and anti-actin.

D   293T cells were transfected with 1.0 µg of pNL4-3 and 0.5 µg of pQCXIP-FLAG-IFITM3 variants. Virus-containing supernatants were harvested and 10 ng p24 equivalents were used to reinfect fresh SupT1 T cells. Productive infection was scored by immunostaining with the KC57 antibody and flow cytometry at 48 h postinfection. Mean + SD of three experiments is shown.

E   About 2.0×10^5 cells were seeded and challenged with 10 ng of HIV-1 NL4-3 in the presence of 2 µg/ml DEAE-dextran. Productive infection was scored by immunostaining with KC57 and flow cytometry at 48 h postinfection. The "Colobus native" sequence represents the full *IFITM3* sequence identified in the colobus monkey.

F   As in (E), except that cells were challenged with influenza A virus (H1N1 PR/8/34, Charles River Laboratories), at a dose that resulted in ~50% infection of control (Empty) cells (equivalent to 10^3 $TCID_{50}$/0.2 ml). Infection was scored by immunostaining with an anti-IAV NP antibody and flow cytometry at 18 h postinfection. Results are presented in a logarithmic scale. Mean + SD of 3–5 experiments is shown.

Data information: Unpaired *t*-test, *$P < 0.05$, **$P < 0.005$.

mutations that govern antiviral potency and specificity are primarily those found among the NEDD4- and AP2-binding motifs.

These results demonstrate that select *IFITM3* sequences derived from nonhuman primates exhibit elevated activity against HIV-1 when expressed in either donor or target cells, suggesting that naturally occurring mutation has led to IFITM3 variants with enhanced anti-lentiviral potential. However, we show that mutations arising in *IFITM3* have opposing effects against HIV-1 and IAV, suggesting a protective trade-off for host antiviral immunity.

Discussion

Despite the conserved antiviral activities displayed by immune-related IFITM proteins, regulatory mechanisms are in place to control their abundance and localization in the cell, allowing for a fine-tuning of the antiviral response. This study identifies the determinants that regulate the potency and specificity with which IFITM3 proteins inhibit HIV-1 infection. We show that post-translational modifications targeting the amino-terminus of IFITM3 impact antiviral activity, and furthermore, the sequence motifs found therein may be subject to natural selection over evolutionary time. Together, these data provide a functional rationale for the recurrent duplication of *IFITM* genes observed in vertebrate genomes. The duplication and subsequent divergence of *IFITM* genes may allow them to be conferred with novel cellular or antiviral functions, a process known as neo-functionalization. Following gene duplication, diversification of *IFITM3* coding sequence via alternative splicing (in the case of the putative Δ1–21 form in humans) or by germ line-encoded codon substitution mutations (in the case of nonhuman primates) may allow the cell to expand its antiviral arsenal and to protect different compartments from viral invaders.

Specifically, our findings suggest that synthetic and naturally occurring mutation of single amino acid residues allows IFITM3 to escape regulation by the E3 ubiquitin ligase NEDD4 and the endocytosis adaptor complex AP-2. However, our description of natural mutations in primate *IFITM3* sequences offers only a first glimpse at the potential variation that exists. It was previously reported that the *IFITM3* locus is duplicated or polymorphic in the rhesus macaque and the African Green Monkey [18,41]. Due to a lack of complete genome sequences, we did not assess *IFITM3* variation in additional members of the primate family *Cercopithicinae*, which comprises most of the monkey species that naturally harbor SIV (and other virus) infections in the wild. Previous reports have demonstrated that these species carry adaptive mutations in restriction factor genes APOBEC3G [42,43], SAMHD1 [44], and TRIM5α [45,46], which impact lentivirus infection *in vitro* and *in vivo*. Thus, cloning of further *IFITM3* genes in diverse species is warranted and may reveal other instances of functional diversification. Future experiments focused on the NEDD4–IFITM3 interaction need to be performed in cells from different tissue types and from different species. For example, while we show that certain primate genomes contain *IFITM3* genes in which the NEDD4-binding site (PPxY) is altered, experiments were performed in human cells (and thus with human NEDD4). It is unknown whether NEDD4 from different species targets the same structural motif as human NEDD4. The prospect that NEDD4 E3 ligases in different species exhibit different substrate specificities is improbable, however, because the NEDD4 homolog in yeast, Rsp5, also targets substrates bearing the same PPxY signature [47]. A departure from this expectation would be exciting, however, since species-specific NEDD4 activities may be indicative of coevolution between NEDD4 and its cellular substrates in a novel form of genetic conflict [37]. Similar questions regarding the cell- or species-specific function of the endocytic adaptor complex, AP-2, must also be addressed.

Previous publications examining the antiviral activity of IFITM3 mutants demonstrated that the hypervariable amino-terminus governs its subcellular localization and, as a result, antiviral activity against IAV. As such, variants of IFITM3 carrying Δ1–21 or ΔY20 were deemed "defective" or "nonfunctional" [20]. On the contrary, we report here that these and other mutations to the amino-terminus of IFITM3 retain and even enhance antiviral function during HIV infection. Furthermore, the use of these hyperactive mutants allowed us to assess the involvement of two distinct, but not mutually exclusive, mechanisms underlying this restriction activity: (i) IFITM3 incorporation into viral membranes and (ii) inhibition of HIV-1 Env maturation and virion incorporation. While our results in 293T cells show that IFITM3 overexpression can lead to slightly decreased gp120 levels in virus-producing cells, as proposed by Yu *et al* [23], we do not observe this phenomenon when IFITM3 is induced in T cells. Previously published studies illustrating an effect of IFITM proteins on the synthesis and maturation of many lentiviral proteins [48], including Gag [17], and even other cellular proteins [49], raise the possibility that IFITM proteins, when overexpressed, promote wholesale changes that may affect protein trafficking in general. Furthermore, an HIV-1 Env-specific effect on restriction activity cannot explain the finding that VSV-G pseudotyping of virions produced in the presence of IFITM proteins does not rescue their infectivity [22]. Overall, while changes to Env may be partially responsible for restriction in 293T cells, our results suggest that the situation may be different in lymphocytes.

The roles played by human IFITM3 in susceptibility to infection have been actively researched, yet many questions remain. Numerous studies have drawn an association between the human SNP rs12252-C in *IFITM3* and a severe outcome to IAV infection, yet the protein variant (Δ1–21) predicted to derive from this SNP has not been directly detected in human cells. Paradoxically, a study has recently reported an association between rs12252-C and rapid progression to AIDS in HIV-infected individuals in China [50]. Since we show here that the Δ1–21 variant exhibits an elevated anti-HIV-1 activity in both of its antiviral roles when ectopically expressed in human cells, efforts are needed to establish a direct functional link between rs12252-C and the truncated protein variant. Importantly, other polymorphisms exist in human *IFITM3*, such as one in the promoter that is associated with susceptibility to tuberculosis [51], further experimental advances will be necessary to directly assess the relationship between genotype, IFITM3 protein, and disease susceptibility. There is evidence for recent positive selection in human *IFITM3* [20], so a scenario whereby "hitchhiking" (linkage disequilibrium) occurs between neighboring SNPs must also be considered.

While mutations to the NEDD4-binding motif (PPxY) did not interfere with anti-IAV function, our description of single amino acid changes and deletions disrupting the endocytosis motif (YxxL)

demonstrates that some naturally occurring mutations carry a cost in the form of a protective trade-off. The recurrent appearance of similar mutations in different primate lineages may reflect the presence of a common selective pressure in the past and may even reveal the nature of the selective pressure itself. Our results suggest that certain nonhuman primate IFITM3 may exhibit greater activity against HIV-1, suggesting that evolution may have fine-tuned their function against lentiviruses or other viruses entering and exiting from the cellular plasma membrane. Future studies examining the activities of primate IFITM3 proteins against their autologous SIV strains will be important for confirming their anti-lentiviral potential and may reveal viral countermeasures that allow antagonism or evasion of IFITM proteins. Regardless, this enhancement of function against lentiviruses comes with a loss of activity against other viruses entering at endosomes, like IAV and VSV. Considering that IFITM3 is critical to the antiviral response to IAV in mice and humans [19,20], the appearance of mutations in nonhuman IFITM3 that suppress this activity is surprising. Thus, our observation that many primate genomes contain multiple *IFITM3* genes may reflect an evolutionary mechanism to provide balanced antiviral protection to the cell. Since some species covered in this study, such as the orangutan, the gorilla, and the common marmoset, have been studied with regard to susceptibility to human virus infections [52,53] it will be of great interest to address how *IFITM3* genotype and gene copy number impact *in vivo* virus replication and transmission.

Materials and Methods

Cells, viruses, and reagents

HEK293T cells (293T, ATCC) and derivatives were cultured in DMEM supplemented with 10% FBS and 1% penicillin–streptomycin. Primary CD4$^+$ T cells and HeLa cells were treated with type-I interferon as previously described [21]. 293T 4 × 4 cells were generated by lentiviral transduction with constructs encoding CD4 and CXCR4, as previously described [40]. pQCXIP plasmids encoding IFITM3 variants with amino-terminal FLAG (FLAG-IFITM3) were previously described [16,17], and additional mutants were generated by site-directed mutagenesis. 293T cells were transfected with Metafectene (Biontex) or Lipofectamine 2000 (Invitrogen) reagent. Tet-ON SupT1 cells were treated with doxycycline (500 ng/ml) overnight to induce FLAG-IFITM3 variants as previously described [16,17,21]. Stocks of HIV-1 were produced via CaPO$_4$ transfection of 293T cells with pNL4-3. HIV-1 incorporating Vpr-B-lactamase (Vpr-Blam) fusion protein was produced via co-transfection of pNL4-3, pVpr-Blam, and pQCXIP encoding IFITM3 variants or an empty control or pCMV-MxA, at a respective plasmid ratio of 3:1.5:1. HIV-1 produced from Tet-ON SupT1 cell lines was produced by first infecting the cells with VSV-G-pseudotyped NL4-3 in the presence of DEAE-dextran (2 μg/ml) followed by overnight doxycycline treatment to induce IFITM3 protein expression.

Western blot

Cells were lysed in 1% Triton-X/PBS in the presence of protease inhibitor cocktail (cOmplete, Roche) and clarified by centrifugation. Virions were purified from supernatants by overlaying on a

6% OptiPrep cushion and pelleted by ultracentrifugation (50,000 × *g*, 4°C) for 1 h. An aliquot was removed for p24 Gag ELISA, and normalized amounts were loaded on a Bis–Tris 12% acrylamide SDS–PAGE gel. The following antibodies were used: mouse anti-FLAG-M2 (Sigma), mouse anti-IFITM3 (Proteintech, 66081-1-Ig), rabbit anti-IFITM3 (Abcam, EPR5242), mouse anti-Gag p24 (183-H12-5C, NIH #1513), sheep anti-Env gp120 (NIH #288), mouse anti-HA (Covance, HA.11 clone 16B12), rabbit anti-actin (Santa Cruz Biotechnology), mouse anti-tubulin (Santa Cruz Biotechnology) and mouse anti-ubiquitin antibody (FK2, Enzo Life Sciences, recognizing K^{29}-, K^{48}-, and K^{63}-linked mono- and poly-ubiquitinated proteins). DyLight-coupled secondary antibodies (Thermo Fisher) were used for protein detection on a Li-Cor Odyssey imaging system.

Flow cytometry

Cells were fixed in 4% PFA and permeabilized with 0.5% saponin. The same antibodies used for Western blot were also used for flow cytometry. In addition, the mouse anti-Gag KC57 (Beckman Coulter) and mouse anti-influenza A group (NP) (Argene) antibodies were used to score HIV-1 and IAV infections, respectively. FLAG M2-PE (Abcam) was used to measure the expression of FLAG-IFITM3 from pQCXIP. Acquisition was performed on a FACS Canto II (Becton Dickinson).

Confocal immunofluorescence microscopy

Transfected 293T cells were cultured on 12-mm glass coverslips, fixed in 4% PFA, and permeabilized with 0.5% saponin. The same antibodies used for Western blot were also used for confocal microscopy. In addition, the mouse anti-p17 Gag (ARP342, AIDS Reagents from Programme EVA Centre) and the mouse anti-LAMP1 (clone H4A3, Santa Cruz Biotechnology) antibodies were used. Analysis was carried out on a Zeiss LSM700 using a 63× objective. Images were analyzed using FIJI software and assembled with the Magic Montage plugin.

Vpr-Blam virus fusion assay

A total of 25 ng p24 equivalent of Vpr-Blam-containing virions was incubated with 1 × 10^5 SupT1 cells. After 2 h, the cells were washed and incubated with the CCF2-AM substrate (CCF2-AM β-lactamase loading kit, Invitrogen) for an additional 2 h. Following fixation in 4% PFA, cleavage of CCF2-AM was measured by flow cytometry.

IFITM3 co-immunoprecipitation and ubiquitination assays

About 5 × 10^5 293T cells were transfected with 0.5 μg pCl-HA-NEDD4 or pCI-HA-NEDD4 C867A and 0.2 μg pQCXIP encoding FLAG-tagged IFITM3 variants. The cells were harvested at 24 h post-transfection and lysed for 30 min on ice in a lysis buffer consisting of 50 mM Tris, 300 mM NaCl, 1 mM EDTA, 1% NP-40, H$_2$O, and a protease inhibitor cocktail. Cell lysates were incubated with prewashed FLAG-M2 agarose beads (Sigma) for 2 h at 4°C. The beads were washed and mixed directly with SDS–PAGE loading buffer (2× Laemmli plus reducing agent). Samples were then denatured by heating at 95°C for 5 min and stored at −20°C until ready for SDS–PAGE loading.

Purification of HIV-1 particles by velocity gradients

About 7×10^6 Tet-ON SupT1 cells (encoding inducible FLAG-IFITM3 or FLAG-IFITM3 Δ1–21) were infected with HIV-1 NL4-3 to achieve approximately 50% Gag$^+$ cells. IFITM3 variants were induced by doxycycline addition (500 ng/ml). After two additional days, supernatants from HIV-1-infected, IFITM3$^+$ cells were filtered on a 0.22-μm filter. Clarified supernatants were ultracentrifuged at $70,000 \times g$ for 1 h. Pellets containing both cellular microvesicles and viral particles were then suspended in PBS and subjected to second ultracentrifugation at $200,000 \times g$ for 1.5 h through a discontinuous 6–18% OptiPrep (iodixanol) gradient, stratified by increments of 1.2%. Ten to eleven fractions were collected and further ultracentrifuged at $435,000 \times g$ for 30 min to concentrate the samples. Pellets were resuspended in 30 μl of 1% Triton-X lysis buffer supplemented with protease inhibitors and directly loaded on a 4–12% acrylamide Bis–Tris SDS–PAGE gel.

Primate *IFITM3* sequence retrieval, molecular analysis, and cloning

IFITM sequences were assembled from reference genome sequences for the following species: mouse lemur (*Microcebus murinus*; micMur1), bushbaby (*Otolemur garnettii*; OtoGar3), tarsier (*Tarsius syrichta*; tarSyr1), common marmoset (*Callithrix jacchus*; C_jacchus3.2.1), rhesus macaque (*Macaca mulatta*; MMUL 1.0), olive baboon (*Papio anubis*; PapAnu2.0), vervet (African Green Monkey-sabeus) (*Chlorocebus sabaeus*; ChlSab1.1), orangutan (*Pongo abelii*; PPYG2), gorilla (*Gorilla gorilla gorilla*; gorGor3.1), chimpanzee (*Pan troglodytes*; CHIMP2.1.4), humans (*Homo sapiens*; GRCh38.p5), and gibbon (*Nomascus leucogenys*; Nleu1.0) using Genomicus v84.01 and Ensembl (www.ensembl.org), with additional sequences provided by BLASTN or BLASTP query in NCBI GenBank. Nucleotide and protein sequence alignments were performed using T-Coffee or Clustal Omega and were adjusted manually in CLC Sequence Viewer. Phylogenetic analysis was performed using the IFITM gene tree function in Ensembl, and the tree visualized consisted of a final consensus tree constructed using distance and maximum-likelihood methods of nucleotide and amino acid sequences. Further phylogenetic analysis was performed using the Bayesian inference method implemented in the MrBayes program (v3.2.3) [54]. Mutations were introduced into the human *IFITM3* sequence by site-directed mutagenesis, while select primate *IFITM3* sequences were directly synthesized by Eurofins Genomics and cloned into the BamHI/EcoRI sites of pQCXIP.

Expanded View for this article is available online.

Author contributions

AAC, CL, JSY, and OS conceived the study. AAC, NR, FP, AB, and NC performed the experiments and data analysis. AAC and OS wrote the manuscript.

Conflict of interest

The authors declare that they have no conflict of interest.

References

1. Bushman FD, Malani N, Fernandes J, D'Orso I, Cagney G, Diamond TL, Zhou H, Hazuda DJ, Espeseth AS, Konig R *et al* (2009) Host cell factors in HIV replication: meta-analysis of genome-wide studies. *PLoS Pathog* 5: e1000437

2. Compton AA, Malik HS, Emerman M (2013) Host gene evolution traces the evolutionary history of ancient primate lentiviruses. *Philos Trans R Soc B Biol Sci* 368: 20120496

3. Chesarino NM, McMichael TM, Hach JC, Yount JS (2014) Phosphorylation of the antiviral protein IFITM3 dually regulates its endocytosis and ubiquitination. *J Biol Chem* 289: 11986 – 11992

4. Sällman Almén M, Bringeland N, Fredriksson R, Schiöth HB (2012) The dispanins: a novel gene family of ancient origin that contains 14 human members. *PLoS One* 7: e31961

5. Blyth GAD, Chan W-F, Webster RG, Magor KE (2015) Duck IFITM3 mediates restriction of influenza viruses. *J Virol* 90: 103 – 116

6. Smith SE, Gibson MS, Wash RS, Ferrara F, Wright E, Temperton N, Kellam P, Fife M (2013) Chicken interferon-inducible transmembrane protein 3 restricts influenza viruses and lyssaviruses *in vitro*. *J Virol* 87: 12957 – 12966

7. Zhu R, Wang J, Lei X-Y, Gui J-F, Zhang Q-Y (2013) Evidence for Paralichthys olivaceus IFITM1 antiviral effect by impeding viral entry into target cells. *Fish Shellfish Immunol* 35: 918 – 926

8. Melvin W, McMichael T, Chesarino N, Hach J, Yount J (2015) IFITMs from mycobacteria confer resistance to influenza virus when expressed in human cells. *Viruses* 7: 3035 – 3052

9. Brass AL, Huang IC, Benita Y, John SP, Krishnan MN, Feeley EM, Ryan BJ, Weyer JL, van der Weyden L, Fikrig E *et al* (2009) The IFITM proteins mediate cellular resistance to influenza a H1N1 virus, West Nile virus, and dengue virus. *Cell* 139: 1243 – 1254

10. Huang IC, Bailey CC, Weyer JL, Radoshitzky SR, Becker MM, Chiang JJ, Brass AL, Ahmed AA, Chi X, Dong L *et al* (2011) Distinct patterns of IFITM-mediated restriction of filoviruses, SARS coronavirus, and influenza a virus. *PLoS Pathog* 7: e1001258

11. Desai TM, Marin M, Chin CR, Savidis G, Brass AL, Melikyan GB (2014) IFITM3 restricts influenza a virus entry by blocking the formation of fusion pores following virus-endosome hemifusion. *PLoS Pathog* 10: e1004048

12. Li K, Markosyan RM, Zheng YM, Golfetto O, Bungart B, Li M, Ding S, He Y, Liang C, Lee JC *et al* (2013) IFITM proteins restrict viral membrane hemifusion. *PLoS Pathog* 9: e1003124

13. Lin TY, Chin CR, Everitt AR, Clare S, Perreira JM, Savidis G, Aker AM, John SP, Sarlah D, Carreira EM *et al* (2013) Amphotericin B increases influenza a virus infection by preventing IFITM3-mediated restriction. *Cell Rep* 5: 895 – 908

14. Amini-Bavil-Olyaee S, Choi YJ, Lee JH, Shi M, Huang IC, Farzan M, Jung JU (2013) The antiviral effector IFITM3 disrupts intracellular cholesterol homeostasis to block viral entry. *Cell Host Microbe* 13: 452 – 464

15. Perreira JM, Chin CR, Feeley EM, Brass AL (2013) IFITMs restrict the replication of multiple pathogenic viruses. *J Mol Biol* 425: 4937 – 4955

16. Jia R, Pan Q, Ding S, Rong L, Liu SL, Geng Y, Qiao W, Liang C (2012) The N-terminal region of IFITM3 modulates its antiviral activity by regulating IFITM3 cellular localization. *J Virol* 86: 13697 – 13707

17. Lu J, Pan Q, Rong L, Liu SL, Liang C (2011) The IFITM proteins inhibit HIV-1 infection. *J Virol* 85: 2126–2137

18. Qian J, Le Duff Y, Wang Y, Pan Q, Ding S, Zheng YM, Liu SL, Liang C (2015) Primate lentiviruses are differentially inhibited by interferon-induced transmembrane proteins. *Virology* 474: 10–18

19. Bailey CC, Huang IC, Kam C, Farzan M (2012) Ifitm3 limits the severity of acute influenza in mice. *PLoS Pathog* 8: e1002909

20. Everitt AR, Clare S, Pertel T, John SP, Wash RS, Smith SE, Chin CR, Feeley EM, Sims JS, Adams DJ *et al* (2012) IFITM3 restricts the morbidity and mortality associated with influenza. *Nature* 484: 519–523

21. Compton AA, Bruel T, Porrot F, Mallet A, Sachse M, Euvrard M, Liang C, Casartelli N, Schwartz O (2014) IFITM proteins incorporated into HIV-1 virions impair viral fusion and spread. *Cell Host Microbe* 16: 736–747

22. Tartour K, Appourchaux R, Gaillard J, Nguyen XN, Durand S, Turpin J, Beaumont E, Roch E, Berger G, Mahieux R *et al* (2014) IFITM proteins are incorporated onto HIV-1 virion particles and negatively imprint their infectivity. *Retrovirology* 11: 103

23. Yu J, Li M, Wilkins J, Ding S, Swartz TH, Esposito AM, Zheng YM, Freed EO, Liang C, Chen BK *et al* (2015) IFITM proteins restrict HIV-1 infection by antagonizing the envelope glycoprotein. *Cell Rep* 13: 145–156

24. Smith SE, Weston S, Kellam P, Marsh M (2014) IFITM proteins—cellular inhibitors of viral entry. *Curr Opin Virol* 4: 71–77

25. Chesarino NM, McMichael TM, Yount JS (2014) Regulation of the trafficking and antiviral activity of IFITM3 by post-translational modifications. *Future Microbiol* 9: 1151–1163

26. Chesarino NM, McMichael TM, Hach JC, Yount JS (2014) Phosphorylation of the antiviral protein interferon-inducible transmembrane protein 3 (IFITM3) dually regulates its endocytosis and ubiquitination. *J Biol Chem* 289: 11986–11992

27. Yount JS, Karssemeijer RA, Hang HC (2012) S-palmitoylation and ubiquitination differentially regulate interferon-induced transmembrane protein 3 (IFITM3)-mediated resistance to influenza virus. *J Biol Chem* 287: 19631–19641

28. Yount JS, Moltedo B, Yang YY, Charron G, Moran TM, López CB, Hang HC (2010) Palmitoylome profiling reveals S-palmitoylation-dependent antiviral activity of IFITM3. *Nat Chem Biol* 6: 610–614

29. Shan Z, Han Q, Nie J, Cao X, Chen Z, Yin S, Gao Y, Lin F, Zhou X, Xu K *et al* (2013) Negative regulation of interferon-induced transmembrane protein 3 by SET7-mediated lysine monomethylation. *J Biol Chem* 288: 35093–35103

30. Jia R, Xu F, Qian J, Yao Y, Miao C, Zheng YM, Liu SL, Guo F, Geng Y, Qiao W *et al* (2014) Identification of an endocytic signal essential for the antiviral action of IFITM3. *Cell Microbiol* 16: 1080–1093

31. Chesarino NM, McMichael TM, Yount JS (2015) E3 ubiquitin ligase NEDD4 promotes influenza virus infection by decreasing levels of the antiviral protein IFITM3. *PLoS Pathog* 11: e1005095

32. Zhang YH, Zhao Y, Li N, Peng YC, Giannoulatou E, Jin RH, Yan HP, Wu H, Liu JH, Liu N *et al* (2013) Interferon-induced transmembrane protein-3 genetic variant rs12252-C is associated with severe influenza in Chinese individuals. *Nat Commun* 4: 1418

33. Xuan Y, Wang LN, Li W, Zi HR, Guo Y, Yan WJ, Chen XB, Wei PM (2015) IFITM3 rs12252 T>C polymorphism is associated with the risk of severe influenza: a meta-analysis. *Epidemiol Infect* 143: 2975–2984

34. Wang Z, Zhang A, Wan Y, Liu X, Qiu C, Xi X, Ren Y, Wang J, Dong Y, Bao M *et al* (2014) Early hypercytokinemia is associated with interferon-induced transmembrane protein-3 dysfunction and predictive of fatal H7N9 infection. *Proc Natl Acad Sci USA* 111: 769–774

35. Herold N, Anders-Osswein M, Glass B, Eckhardt M, Muller B, Krausslich HG (2014) HIV-1 entry in SupT1-R5, CEM-ss, and primary CD4+ T cells occurs at the plasma membrane and does not require endocytosis. *J Virol* 88: 13956–13970

36. Zhu X, He Z, Yuan J, Wen W, Huang X, Hu Y, Lin C, Pan J, Li R, Deng H *et al* (2014) IFITM3-containing exosome as a novel mediator for anti-viral response in dengue virus infection. *Cell Microbiol* 17: 105–118

37. Duggal NK, Emerman M (2012) Evolutionary conflicts between viruses and restriction factors shape immunity. *Nat Rev Immunol* 12: 687–695

38. Zhang Z, Liu J, Li M, Yang H, Zhang C (2012) Evolutionary dynamics of the interferon-induced transmembrane gene family in vertebrates. *PLoS One* 7: e49265

39. Louis A, Muffato M, Roest Crollius H (2013) Genomicus: five genome browsers for comparative genomics in eukaryota. *Nucleic Acids Res* 41 (Database issue): D700–D705

40. Lepelley A, Louis S, Sourisseau M, Law H, Pothlichet J, Schilte C, Chaperot L, Plumas J, Randall RE, Si-Tahar M *et al* (2011) Innate sensing of HIV-infected cells. *PLoS Pathog* 7: e1001284

41. Wrensch F, Karsten CB, Gnirss K, Hoffmann M, Lu K, Takada A, Winkler M, Simmons G, Pohlmann S (2015) Interferon-induced transmembrane protein-mediated inhibition of host cell entry of ebolaviruses. *J Infect Dis* 212(Suppl. 2): S210–S218

42. Compton AA, Emerman M (2013) Convergence and divergence in the evolution of the APOBEC3G-Vif interaction reveal ancient origins of simian immunodeficiency viruses. *PLoS Pathog* 9: e1003135

43. Krupp A, McCarthy KR, Ooms M, Letko M, Morgan JS, Simon V, Johnson WE (2013) APOBEC3G polymorphism as a selective barrier to cross-species transmission and emergence of pathogenic SIV and AIDS in a primate host. *PLoS Pathog* 9: e1003641

44. Spragg CJ, Emerman M (2013) Antagonism of SAMHD1 is actively maintained in natural infections of simian immunodeficiency virus. *Proc Natl Acad Sci* 110: 21136–21141

45. McCarthy KR, Kirmaier A, Autissier P, Johnson WE (2015) Evolutionary and functional analysis of old world primate TRIM5 reveals the ancient emergence of primate lentiviruses and convergent evolution targeting a conserved capsid interface. *PLoS Pathog* 11: e1005085

46. Kirmaier A, Wu F, Newman RM, Hall LR, Morgan JS, O'Connor S, Marx PA, Meythaler M, Goldstein S, Buckler-White A *et al* (2010) TRIM5 suppresses cross-species transmission of a primate immunodeficiency virus and selects for emergence of resistant variants in the new species. *PLoS Biol* 8: e1000462

47. Gupta R, Kus B, Fladd C, Wasmuth J, Tonikian R, Sidhu S, Krogan NJ, Parkinson J, Rotin D (2007) Ubiquitination screen using protein microarrays for comprehensive identification of Rsp5 substrates in yeast. *Mol Syst Biol* 3: 1–12

48. Chutiwitoonchai N, Hiyoshi M, Hiyoshi-Yoshidomi Y, Hashimoto M, Tokunaga K, Suzu S (2013) Characteristics of IFITM, the newly identified IFN-inducible anti-HIV-1 family proteins. *Microbes Infect* 15: 280–290

49. Wee YS, Roundy KM, Weis JJ, Weis JH (2012) Interferon-inducible transmembrane proteins of the innate immune response act as membrane organizers by influencing clathrin and v-ATPase localization and function. *Innate Immun* 18: 834–845

50. Zhang Y, Makvandi-Nejad S, Qin L, Zhao Y, Zhang T, Wang L, Repapi E, Taylor S, McMichael A, Li N *et al* (2015) Interferon-induced transmembrane protein-3 rs12252-C is associated with rapid

progression of acute HIV-1 infection in Chinese MSM cohort. *AIDS* 29: 889–894

51. Shen C, Wu XR, Jiao WW, Sun L, Feng WX, Xiao J, Miao Q, Liu F, Yin QQ, Zhang CG *et al* (2013) A functional promoter polymorphism of IFITM3 is associated with susceptibility to pediatric tuberculosis in Han Chinese population. *PLoS One* 8: e67816

52. Buitendijk H, Fagrouch Z, Niphuis H, Bogers W, Warren K, Verschoor E (2014) Retrospective serology study of respiratory virus infections in captive great apes. *Viruses* 6: 1442–1453

53. Moncla LH, Ross TM, Dinis JM, Weinfurter JT, Mortimer TD, Schultz-Darken N, Brunner K, Capuano SV III, Boettcher C, Post J *et al* (2013) A novel nonhuman primate model for influenza transmission. *PLoS One* 8: e78750

54. Ronquist F, Huelsenbeck JP (2003) MrBayes 3: Bayesian phylogenetic inference under mixed models. *Bioinformatics* 19: 1572–1574

55. De Bie T, Cristianini N, Demuth JP, Hahn MW (2006) CAFE: a computational tool for the study of gene family evolution. *Bioinformatics* 22: 1269–1271